Research Article

Galleria mellonella as an Alternative *In Vivo* Model to Study Bacterial Biofilms on Stainless Steel and Titanium Implants

Gopala K. Mannala[1], Markus Rupp[1], Francisca Alagboso[1], Maximilian Kerschbaum[1], Christian Pfeifer[1], Ursula Sommer[2], Marian Kampschulte[3], Eugen Domann[4] and Volker Alt[1]

[1]Department of Trauma Surgery, University Hospital Regensburg, Regensburg, Germany; [2]Experimental Trauma Surgery, Justus Liebig University Giessen, Giessen, Germany; [3]Department of Radiology, University Hospital Giessen-Marburg, Campus Giessen, Giessen, Germany; [4]Institute for Medical Microbiology, Biomedizinisches Forschungzentrum Seltersberg (BFS), Giessen, Germany

Abstract

The purpose of this study was to establish an infection model of *Galleria mellonella* larvae as an alternative *in vivo* model for biofilm-associated infections on stainless steel and titanium implants. First, the model was established with sterile implants to evaluate biocompatibility. Titanium or stainless steel implants were implanted without adverse effects over the entire observation period of 5 days compared to controls and even up to the pupae and moth stage. Then, stainless steel and titanium implants contaminated with *Staphylococcus aureus* were implanted into larvae to mimic biofilm-associated infection. For both materials, pre-incubation of the implant with *S. aureus* led to significantly reduced survival of the larvae compared to sterile implants. Larvae could not be rescued by gentamicin, whereas gentamicin significantly improved the survival of the larvae in case of planktonic infection with *S. aureus* without an implant, confirming the typical characteristics of reduced antibiotic susceptibility of biofilm infections. Biofilm formation and various stages of biofilm maturation were confirmed by surface electron microscopy and by measuring bacterial gene expression of biofilm-related genes on contaminated implants, which confirmed biofilm formation and upregulation of autolysin (*atl*) and *sarA* genes. In conclusion, *G. mellonella* can be used as an alternative *in vivo* model to study biofilm-associated infections on stainless steel and titanium implants, which may help to reduce animal infection experiments with vertebrates in the future.

1 Introduction

Progress in medical research has led to the development of a multitude of implantable medical devices. Their extensive use in clinical routine as metal or ceramic prostheses, catheters or heart valves, to mention only a few, has strongly contributed to the success story of modern medicine (Bechert et al., 2000; Waldvogel, 2000). However, colonization of medical devices with pathogens, eventually forming biofilm on implant surfaces, is a common, critical problem. After a biofilm is formed, medical antibiotic or antimycotic treatment often fails due to manifold bacterial defense mechanisms (Zimmerli et al., 2004; Ribeiro et al., 2012). Hence, biofilms established on medical devices often require removal of the implant to achieve eradication of the infection. The impact of such surgical procedures for removal and, often, reimplantation after eradication of the infection is high, both for the individual patient and with respect to costs (Zimmerli et al., 2004).

Several *in vitro* and *in vivo* models have been developed to study the process of biofilm formation (Lebeaux et al., 2013). In translational research, *in vivo* models such as rat, rabbit, dog and sheep are widely used to assess the biocompatibility of orthopedic implants as well as to test antimicrobial coatings and compounds against biofilm formation caused by various microorganisms.

In general, vertebrate models are restricted in use for scientific purposes due to animal welfare and ethical reasons. This is particularly true for infection experiments such as to study biofilm formation and treatment, as inoculation of bacteria or other microorganisms often results in a high burden of disease in the animals (Moriarty et al., 2019). Therefore, ethical approval is usually restricted. To provide best possible protection of re-

Received March 21, 2020; Accepted October 15, 2020;
Epub October 21, 2020; © The Authors, 2021.

ALTEX 38(2), 245-252. doi:10.14573/altex.2003211

Correspondence: Prof. Dr med. Dr biol. hom. Volker Alt
Department of Trauma Surgery, University Hospital Regensburg
Franz-Josef-Strauß-Allee 11, 93053 Regensburg, Germany
(volker.alt@ukr.de)

search animals, each research project should implement the 3R (replacement, reduction, refinement) principles introduced by Russell and Burch (1959).

In recent decades, invertebrates such as *Drosophila melanogaster*, *Caenorhabditis elegans* and *Galleria mellonella* have been widely used as infection models to study host-pathogen interactions as well as virulence of bacterial and fungal pathogens (Mukherjee et al., 2010; Mannala et al., 2017a, 2018). In addition, they have enabled testing of the antimicrobial activity of drugs. These models are economical, have no ethical issues and are easy to handle. Among them, the larva of the greater wax moth, *G. mellonella*, has been used extensively to test the virulence of bacterial pathogens. Recently, our group evaluated virulence levels of various clinically relevant *Staphylococcus aureus* strains isolated from implant-associated infections using this model (Mannala et al., 2018). Earlier, *G. mellonella* also was used to assess accumulation of bacterial pathogens on different toothbrush bristles to mimic biofilm infections on a foreign body. After piercing the larva proleg with the bristles, the signs of infection were observed, bacteria enumerated and biofilm analyzed by SEM (Benthall et al., 2015; Campos-Silva et al., 2019).

To our knowledge, orthopedic metallic implants have not yet been used in *G. mellonella* to study implant-associated infections and bacterial biofilm formation. The aim of the current study was the establishment of this insect infection model for biofilm-associated infections for stainless steel and titanium implants in order to mimic biofilm infections following orthopedic surgery. For this purpose, the biocompatibility of the implants was assessed first. Then the effects of implants that had been contaminated with *S. aureus* and the effects of treatment with gentamicin on *G. mellonella* survival, as well as the changes in implant-associated bacterial gene expression and biofilm morphology were evaluated.

2 Animals, materials and methods

Larvae, bacteria, growth conditions and preparation of implants
G. mellonella larvae were obtained from Fauna Topics GmbH (Rielingshausen, Germany) and maintained on an artificial diet in an incubator at 30°C. For each experiment, 10 larvae in the last instar stage weighing 200-250 mg were used. After infection, *G. mellonella* were maintained at 37°C.

Staphylococcus aureus strain EDCC 5055 was used for infection experiments. This strain is known for its high biofilm formation capacity and its whole genome sequence is available (Mannala et al., 2017b, 2018). Brain-heart-infusion (BHI) broth was used to maintain *S. aureus* aerobically at 37°C by constant shaking at 180 rpm. An overnight culture was diluted 1:50 and grown to mid-exponential phase with an optical density of 1.0 at 600 nm. The culture was then washed twice with saline solution (0.9% NaCl). The bacterial concentration in colony forming units (CFU) per mL was adjusted with saline solution based on the optical density.

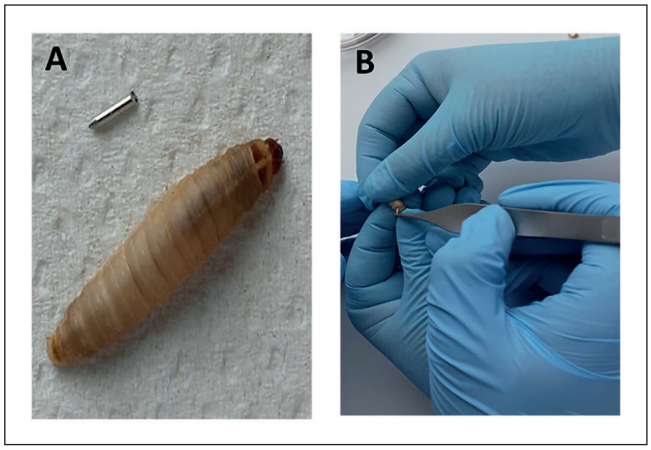

Fig. 1: Preparation of larvae and implants and the implantation process
(A) Stainless steel or titanium implants with a length of 4-5 mm and 0.8 mm diameter with one sharp-edged side were implanted in larvae weighing 200-250 mg. (B) The implants were inserted inside the larvae with the help of tweezers. The larvae were held by one person, and another person pierced the cuticle of the segmented region (rear part of the larvae) with the sharp-edged part and pushed it completely into the body of the larvae. Further details can be seen in the supplementary video[1]

Sterile stainless steel and titanium K-wires with a diameter of 0.8 mm (Synthes, Zuchwil, Switzerland) were used as implant materials. Pieces with a length of 4-5 mm were cut with a cable cutter, and one end was sharpened using a sharpener (Fig.1).

Establishment of the G. mellonella *implant model*
The larvae were held by one person, and another person implanted the K-wire using metal tweezers. The implants were placed in the rear part of the larvae by piercing the cuticle with the sharp edge of the implant material and pushing the K-wire inside. For easy piercing and implantation, it is recommended to implant at the segmented region where the cuticle is thinner (see supplementary video[1]). Control larvae were injected with 10 µl saline solution. After implantation, the larvae were placed in Petri dishes containing artificial diet at 30°C and observed for activity and survival for 5 days or until the pupae and subsequent moth stages. Metal toxicity would lead to reduced activity and death of the larvae. Wound healing and melanization at the implantation site were assessed based on the leaking of hemolymph or pus generation and the change of skin color. These parameters were used to assess the implantation success and the biocompatibility of the implants.

Micro-CT analysis
Cross-sectional imaging was performed using a SkyScan 1173 micro-CT system (Bruker microCT, Kontich, Belgium) equipped

[1] doi:10.14573/altex.2003211s1

with a high voltage tube for imaging of dense materials. Larvae were wrapped in parafilm and mounted on a rotational stage for *ex vivo* scanning. Cross sectional images were reconstructed by filtered back projection using the NRecon software (Version: 1.7.1.0, Bruker microCT, Kontich, Belgium). Image acquisition and reconstruction parameters are described in Table S1[2].

Infection experiments with pre-incubated stainless steel and titanium implants in bacterial suspension

Implants were pre-incubated with 1x10^6 CFU/mL *S. aureus* for 30 min under shaking at 150 rpm. Then, the implants were washed with 10 mL PBS and implanted in the larvae as described above. For the control groups, the same process was followed but without bacterial contamination of the implants.

To determine the number of adherent bacteria before implantation, implants were sonicated in PBS at 40 kHz, 0.1-1 W/cm^2 in a sonication bath for 1 min and vortexed for 1 min. The suspension was plated on Luria-Bertani (LB) agar plates. Bacterial colonies were counted after incubation of plates at 37°C for 16 h.

Ten larvae were used for each group, and each experiment was repeated at least 3 times.

Planktonic infection without implants and effects of gentamicin

In order to distinguish the *S. aureus* biofilm infection on the implants from a planktonic infection with *S. aureus* without an implant, larvae were injected with 4,000 CFUs *S. aureus*. This bacterial load corresponded to that of the adherent bacteria determined on the metallic surface of the stainless steel and titanium implants used for the biofilm infection model. Survival rates were compared.

In order to determine the effect of gentamicin on survival in the biofilm infection model using stainless steel implants and in the planktonic infection model, the larvae were injected with gentamicin (120 mg/kg) on day 1 after insertion of the *S. aureus* contaminated implant or after planktonic infection. All experiments were run 3 times.

Scanning electron microscopy

For SEM analysis, implants were extracted from larvae at specified time points, washed twice in PBS to remove planktonic cells, and fixed with 1% sucrose and 2.5% glutaraldehyde at 4°C for 24 h. Thereafter, samples were washed 6 times with PBS and dehydrated with lower to higher ethanol concentrations (30%, 50%, 70%, 80%, and 96%) for 15 min each, then 3 times with 100% ethanol for 30 min. Samples were dried in a critical point dryer (Leica EM CPD300) and sputter-coated with gold and palladium (Polaron Sputter Coater SC7640). Analysis was performed in a LEO1530 at 15 kV. The biofilm formation on day 2 was analyzed on both stainless steel and titanium implants. Biofilm maturation was analyzed on the stainless steel implants on days 1-4. Four samples of each setting were analyzed.

RNA isolation and qRT-PCR analysis

RNA was extracted from 0.5 mL aliquots of the *S. aureus* culture grown extracellularly in BHI until mid-exponential phase that was used for infection experiments. The bacterial cells were treated with 1.0 mL RNA protect (Qiagen) for 5 min and were collected by centrifugation for 10 min (8000 g). The bacterial pellets were stored at -80°C until use. For RNA extraction from the biofilms, the implants were extracted from the larvae on day 2, sonicated, pelleted by centrifugation, and stored at -80°C. Total RNA was isolated using miRNeasy kit (Qiagen, Hilden, Germany) with some modifications.

The collected bacterial pellets were washed with SET buffer (50 mM NaCl, 5 mM EDTA and 30 mM Tris-HCl, pH 7.0) by centrifugation at 16,000 g for 3 min. After wash steps, pellets were resuspended in 0.1 mL Tris-HCl (pH 6.5) containing 50 mg/mL lysozyme (Sigma), 25 U mutanolysin (Sigma), 40 U SUPERase (Ambion), and 0.2 mg proteinase K (Ambion). The suspension was incubated for 30 min on a thermomixer at 37°C under shaking at 350 rpm. Lysis of the cell suspension was performed by addition of QIAzol (Qiagen) followed by mixing and incubation for 3 min at room temperature. 0.2 volumes of chloroform were added to the suspension, mixed well and centrifuged at 16,000 g at 4°C for 15 min. The upper aqueous phase containing RNA was collected into a new collection tube and 1.5 volumes of 100% ethanol were added and mixed thoroughly. The samples containing RNA were transferred into columns of the miRNeasy Kit (Qiagen, Hilden, Germany) and underwent on-column DNase digestion (RNase-Free DNase, Qiagen). RNA was eluted with RNase-free water and stored at -20°C until needed. The RNA quantity was determined by absorbance at 260 nm and 280 nm, and the quality was assessed using Nano-chips on an Agilent 2100 Bioanalyzer.

Reverse transcription was performed by SuperScript II Reverse Transcriptase (Invitrogen) using 1 µg RNA. The samples were processed for quantitative real-time PCR in a final volume of 25 µL using QuantiTect SYBR Green PCR kit (Qiagen) according to the manufacturer's instructions. A standard curve was generated for all used primer pairs (see Tab. S2[2]) using different copy numbers of genomic DNA from *S. aureus* EDCC 5055. For each primer pair, a negative control (water) and an RNA sample that had not undergone the reverse transcription reaction (for genomic DNA contamination) were included as controls during cDNA quantification. After real-time PCR, all samples were run on a 1.5% agarose gel to confirm that only a single band was produced. The expression level of each gene was measured by normalizing to *gyrB* for the same sample using the formula for relative quantification in real-time PCR published by Pfaffl (2001).

Statistical analysis

Statistical analysis of the data was performed using SigmaPlot 10.0. For the survival analysis, two-way ANOVA was performed. For the analysis of qRT-PCR, Student's t-test was applied. The data is represented as means ± standard deviation of

[2] doi:10.14573/altex.2003211s2

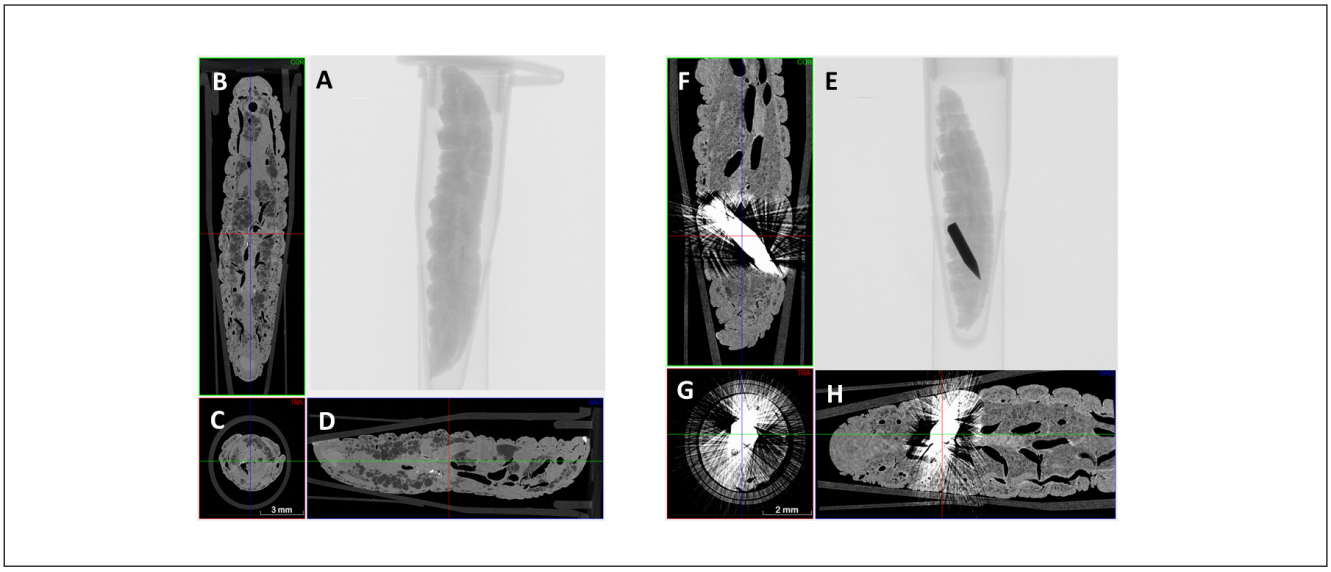

Fig. 2: Micro-CT cross-sectional imaging of larvae
Typical *G. mellonella* anatomy (A-D). The larva shows a fully inserted implant in the rear part of its body (E-H).

three independent experiments. The data was considered significant if the p-value was < 0.05.

3 Results

3.1 Biocompatibility of *G. mellonella* implants

The implantation procedure was established successfully, and micro-CT demonstrated intra-body location of the implant inside the larvae in all cases (Fig. 2). The larvae with implants were similarly active to the control group, which had been saline-treated and their survival rate was above 90% five days after implantation (Fig. 3). The implantation of stainless steel or titanium implants did not cause any adverse effects such as metal toxicity, wound healing disturbances or melanization at the site of implantation. No effects were detected on the life stages of *G. mellonella* larvae, as the implanted metals could be detected in pupae and moth stages (Fig. S1[2]).

3.2 *G. mellonella* as implant-associated *S. aureus* biofilm infection model

Determination of total adherent bacteria on contaminated implants before implantation revealed comparable bacterial numbers between stainless steel (4,000 ± 700 CFUs) and titanium (3,800 ± 500 CFUs) implants. The number of adherent bacteria per area on the stainless steel and titanium K-wires was 137/mm^2 and 130/mm^2, respectively.

Fig. 4 shows the survival curves of the larvae implanted with *S. aureus* contaminated stainless steel and titanium K-wires. The larvae showed a significantly lower 5-day survival after implantation of *S. aureus* contaminated stainless steel (5-day survival: 27 ± 3.5%) or titanium implants (5-day survival: 47 ± 3.5%) compared to respective controls (steel: 90 ± 0.0%, titanium: 95 ± 7.0%) (p < 0.001).

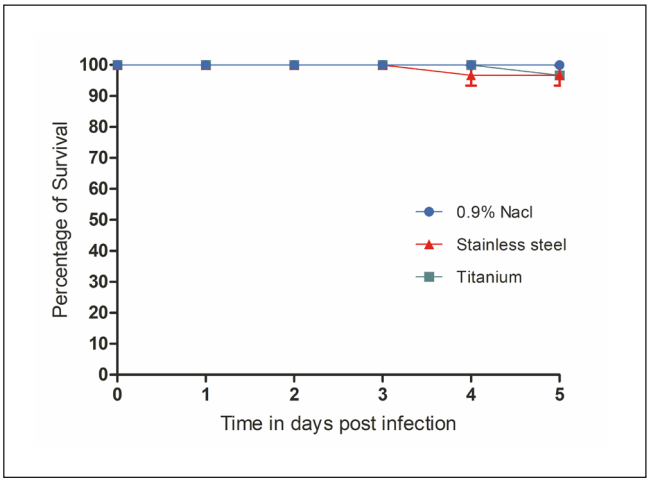

Fig. 3: Survival of *G. mellonella* with titanium or stainless steel implants
No significant differences are seen between the survival rates of saline-treated larvae and larvae implanted with sterile stainless steel or titanium K-wires. Experiments were conducted with 10 larvae per group. The data is represented as means ± standard deviation from three independent experiments.

3.3 Comparison between implant-associated biofilm infection and planktonic infection and rescue by gentamicin

Larvae that were infected with planktonic *S. aureus* showed a higher survival rate, particularly in the first 4 days, compared to larvae infected with stainless steel implants contaminated with the same number of bacteria. Gentamicin did not rescue larvae

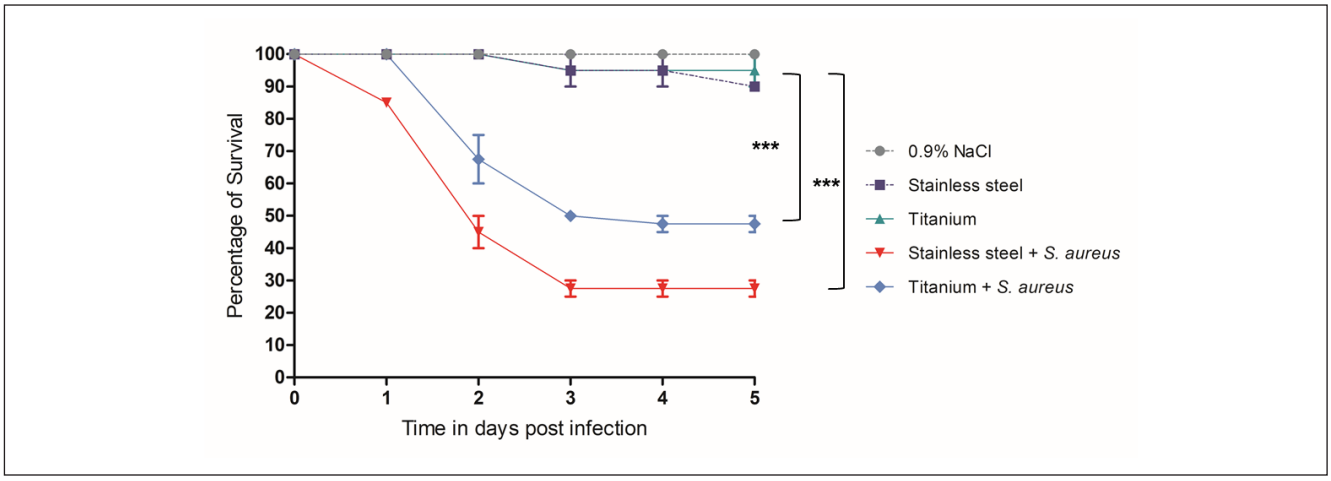

Fig. 4: Survival of *G. mellonella* with titanium and stainless steel implants that were contaminated with *S. aureus*
Larvae that received contaminated implants showed a significantly reduced survival rate compared to larvae with sterile implants, both for titanium and for stainless steel implants (***p ≤ 0.001, two-way ANOVA). The data are presented as means ± standard deviation from three independent experiments; experiments were conducted with 10 larvae per group.

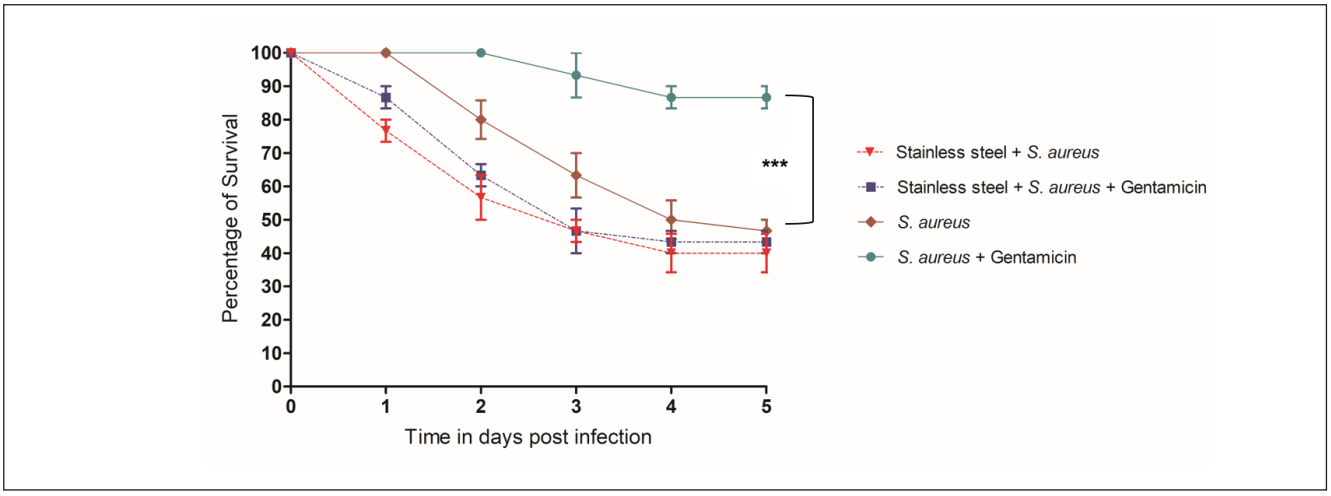

Fig. 5: Comparison between biofilm infection and planktonic infection and rescue by gentamicin
Larvae that were infected with *S. aureus* without an implant (planktonic infection model) showed a higher survival rate, particularly in the first 4 days, compared to the biofilm infection model with contaminated stainless steel implants. Gentamicin did not rescue the larvae with contaminated implants, whereas gentamicin significantly improved survival in the planktonic infection model (***p < 0.001, two-way ANOVA). The data are presented as means ± standard deviation from three independent experiments; experiments were conducted with 10 larvae per group.

with implant-associated biofilm infection, whereas it significantly improved survival of the planktonic infection ($p < 0.001$) (Fig. 5).

3.4 RNA isolation and qRT-PCR analysis

To study changes in biofilm-related gene expression, RNA was isolated from the extracellular culture as well as the biofilm formed 2 days after implantation of contaminated K-wires on day 2. Among the tested genes, *atl*, *sarA*, and *icaA* genes were significantly upregulated whereas *fib*, *fnbB* and *fnbA* genes were significantly downregulated in the biofilm versus extracellular bacteria. No changes in the expression of *clfB* and *agrA* genes were observed. Among the upregulated genes, autolysin (*atl*) showed a 6-fold upregulation, *sarA* a 3-fold and *icaA* a 2-fold upregulation (Fig. 6).

3.5 Biofilm visualization on implants with SEM analysis

Figure 7 shows the biofilm formation on the surface of both the titanium and stainless steel implants with *S. aureus* bacteria on day 2 after implantation. Cell-to-cell adherence and clump formation features, which are typical features of biofilm, are clearly visible. To follow the biofilm maturation over time, SEM analysis was performed on stainless steel implants that were explanted

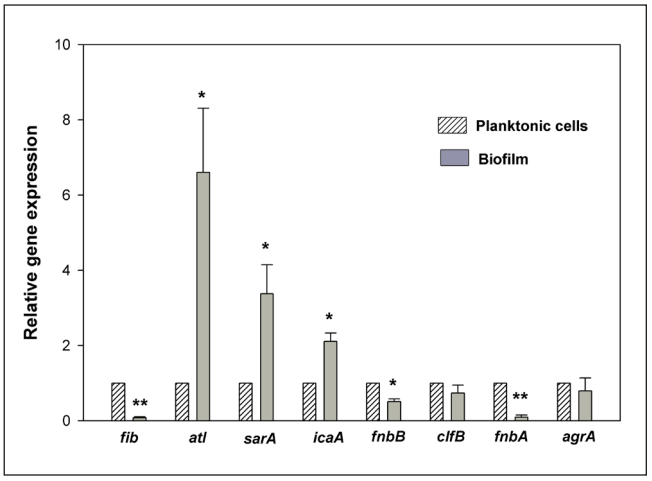

Fig. 6: Biofilm-related gene expression analysis
To investigate key genes involved in biofilm formation, qRT-PCR analysis was performed in samples from extracellular bacteria and biofilms. Among these, autolysin (*atl*), *sarA* and *icaA* were significantly upregulated (*p ≤ 0.05; t-test), and fibrin (*fib*) and fibronectin binding proteins (*fnbA* and *fnbB*) were significantly downregulated (*p ≤ 0.05, **p ≤ 0.01; t-test). No changes in gene expression levels were observed for *clfB* and *agrA* genes.
The data are represented as means ± standard deviation from three independent experiments.

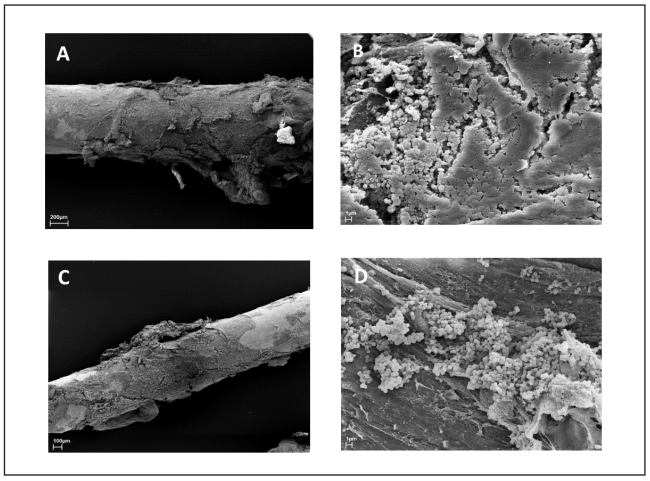

Fig. 7: Biofilm visualization on implants by SEM analysis
Two days after implantation, *S. aureus*-contaminated implants were extracted and processed for SEM analysis. Representative SEM images of biofilm formed on stainless steel (A+B) and on titanium (C+D) implants show bacterial cell-to-cell attachments. Images A and C were taken at a magnification of 2000X (scale bar: 200 μm and scale bar: 100 μm, respectively); B and D were taken at a magnification of 10,000X (scale bar: 1 μm). Four samples were analyzed for each setting.

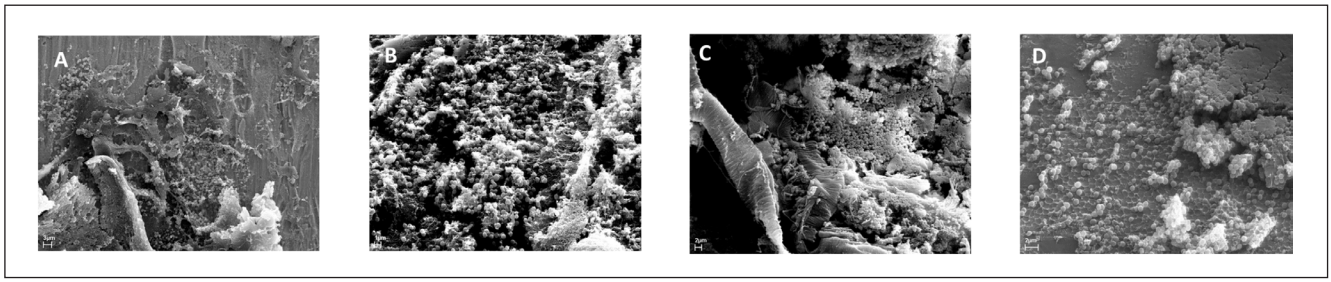

Fig. 8: Visualization of biofilm maturation stages with SEM
S. aureus-contaminated stainless steel implants were extracted on days 1 to 4 and processed for SEM analysis. Representative SEM images of biofilm maturation with attachment of bacteria to surface on day 1 (A) (10,000X; scale bar: 1 μm), accumulation of bacteria on day 2 (B) (10,000X; scale bar: 3 μm), maturation of biofilm on day 3 (C) (10,000X; scale bar: 2 μm), and dispersal or removal of biofilm on day 4, leaving empty lacunae on the implant surface (D) (10,000X; scale bar: 2 μm). Four samples were analyzed for each setting.

from larvae on days 1 to 4 after implantation. The images show attachment of bacteria (Fig. 8A), accumulation (Fig. 8B), maturation (Fig. 8C), and detachment or reduction of biofilm mass, likely due to an immune response, leaving empty lacunae on the implant surface (Fig. 8D).

4 Discussion

G. mellonella has been previously used to evaluate biofilm-related infections with a foreign material using different tooth brush bristles (Benthall et al., 2015; Campos-Silva et al., 2019). However, to our knowledge, metallic implants were not studied in this insect model before. The main aim of the current work was to establish and to evaluate a *G. mellonella* biofilm infection model of stainless steel and titanium implants to model biofilm infections after orthopedic surgery. Our results demonstrate that *G. mellonella* is a suitable model to study biofilm infections with stainless steel and titanium implants, as it shows the major characteristics of biofilm infection on metallic surfaces.

Success of the implantation procedure and biocompatibility of the metallic implants was shown. The implantation was performed by piercing the cuticle without any adverse effects to the larvae, such as hemolymph bleeding, toxic effects or melaniza-

tion. The larvae tolerated the implanted metallic implants over the entire observation period with only a slight reduction of survival rate compared to saline-treated larvae. The implants remained integrated in the course of all stages of the *G. mellonella* life cycle, including pupae and moth. These results indicate that the metallic implants are well tolerated in the larvae system.

Implants contaminated with *S. aureus* caused a significant reduction in survival of the larvae compared to sterile implants. The model exhibited typical characteristics of a biofilm infection, which is generally associated with reduced susceptibility to antibiotics compared to a planktonic infection (Benthall et al., 2015), as gentamicin did not rescue the biofilm infection model, whereas it was highly effective in the planktonic model, significantly improving survival.

Both titanium and stainless steel implants that were contaminated with bacteria exhibited characteristic biofilm formation on their surface as shown by SEM analysis. All typical stages of biofilm formation as described by others in previous studies (Joo and Otto, 2012; Nishitani et al., 2015; Khatoon et al., 2018), including attachment, accumulation, maturation and dispersal of bacteria from biofilm, were found. In comparison to results of biofilm studies in a mouse model described by Nishitani et al. (2015), the biofilm was already dispersed on day 4 in our model while this only occurred at day 14 post infection in the mouse model. This might be due to the shorter life cycle of the larvae or differences in the immune response between these two species.

S. aureus biofilm formation is known to be mainly regulated by two genetic loci, namely *sarA* (staphylococcal accessory regulator) and the agr quorum sensing system (Balamurugan et al., 2017). Several *in vitro* and *in vivo* studies have revealed that *sarA* is involved in biofilm formation by regulation of several biofilm-related genes (Yarwood et al., 2004; Valle et al., 2007). In line, *sarA* mutants are known to result in defective biofilm formation (Beenken et al., 2003; Tsang et al., 2008). The agr quorum sensing system functions by sensing *S. aureus* growth through extracellular levels of autoinducing peptides (AIPs) (Le and Otto, 2015) and is known for its role in the initiation and regulation of biofilm formation and the dispersal of biofilms (Paharik and Horswill, 2016). Several studies have reported that clumping factor B (*clfB*), fibrin coding gene (*fib*) and fibronectin binding protein coding genes (*fnbA* and *fnbB*) are upregulated in *S. aureus* biofilms (Kot et al., 2018; Azmi et al., 2019). Autolysin (*atl*) is a key gene in the context of bacterial attachment to foreign body surfaces (Dai et al., 2012; Khatoon et al., 2018).

In the current study, we analyzed the changes in gene expression during biofilm formation in comparison to extracellularly grown bacteria. As expected, *atl* was shown to be relatively highly expressed in biofilm-associated bacteria in comparison to extracellularly grown bacteria. The biofilm regulatory molecules *sarA* and intracellular adhesion protein (*icaA*) were upregulated as well, which is in line with similar findings in the literature (Khatoon et al., 2018; Moriarty et al., 2019). The quorum sensing system gene *agrA* did not show changes in gene expression levels. Interestingly, fibrin coding gene (*fib*) and fibronectin binding protein coding genes (*fnbA* and *fnbB*) were downregulated, whereas clumping factor B (*clfB*) was not modulated in the presented model. This might be due to a lack of fibrin and fibronectin proteins in *G. mellonella* and may be a limitation of the model.

The model is of relevance due to its low cost and its potential for high throughput analysis, e.g., for screening of antimicrobial materials, such as coatings or other anti-infective treatment strategies. It avoids, application and decision processes of animal welfare committees, which are sometimes complicated and time-consuming as well as most ethical issues in this relation, while still representing an intact organism.

The model has some limitations, especially that *Galleria* lacks an adaptive immune system and has a short life cycle that does not allow the study of chronic infections. The absence of a skeletal system excludes typical bone-associated reactions and may limit conclusions on orthopedic implants. Furthermore, although the use of animals protected by legislation, i.e. vertebrates, can be reduced by this model, it does also rely on a living organism.

Future studies can assess whether the application of this model can be expanded to include further relevant materials such as polyethylene (PE) or polymethylmethacrylate (PMMA) and different causative agents apart from *S. aureus*. In a next step, a direct comparison between this model and a clinically relevant orthopedic infection model, e.g., infected non-unions in rats (Alt et al., 2011) or others (Moriarty et al., 2017), should be conducted.

5 Conclusion

In conclusion, our results show that *G. mellonella* can be used as an alternative *in vivo* model to study biofilm-associated infections on stainless steel and titanium implants and assess potential treatment methods, which may help to reduce animal infection experiments with vertebrates in the future.

References

Alt, V., Lips, K. S., Henkenbehrens, C. et al. (2011). A new animal model for implant-related infected non-unions after intramedullary fixation of the tibia in rats with fluorescent in situ hybridization of bacteria in bone infection. *Bone 48*, 1146-1153. doi:10.1016/j.bone.2011.01.018

Azmi, K., Qrei, W. and Abdeen, Z. (2019). Screening of genes encoding adhesion factors and biofilm production in methicillin resistant strains of Staphylococcus aureus isolated from Palestinian patients. *BMC Genomics 20*, 578. doi:10.1186/s12864-019-5929-1

Balamurugan, P., Praveen Krishna, V., Bharath, D. et al. (2017). Staphylococcus aureus quorum regulator SarA targeted compound, 2-[(Methylamino)methyl]phenol inhibits biofilm and down-regulates virulence genes. *Front Microbiol 8*, 1290. doi: 10.3389/fmicb.2017.01290

Bechert, T., Steinrücke, P. and Guggenbichler, J. P. (2000). A new method for screening anti-infective biomaterials. *Nat Med 6*, 1053-1056. doi:10.1038/79568

Beenken, K. E., Blevins, J. S. and Smeltzer, M. S. (2003). Mutation of sarA in Staphylococcus aureus limits biofilm forma-

tion. *Infect Immun 71*, 4206-4211. doi:10.1128/IAI.71.7.4206-4211.2003

Benthall, G., Touzel, R. E., Hind, C. K. et al. (2015). Evaluation of antibiotic efficacy against infections caused by planktonic or biofilm cultures of Pseudomonas aeruginosa and Klebsiella pneumoniae in Galleria mellonella. *Int J Antimicrob Agents 46*, 538-545. doi:10.1016/j.ijantimicag.2015.07.014

Campos-Silva, R., Brust, F. R., Trentin, D. S. et al. (2019). Alternative method in Galleria mellonella larvae to study biofilm infection and treatment. *Microb Pathog 137*, 103756. doi:10.1016/j.micpath.2019.103756

Dai, L., Yang, L., Parsons, C. et al. (2012). Staphylococcus epidermidis recovered from indwelling catheters exhibit enhanced biofilm dispersal and "self-renewal" through down-regulation of agr. *BMC Microbiol 12*, 102. doi:10.1186/1471-2180-12-102

Joo, H. S. and Otto, M. (2012). Molecular basis of in vivo biofilm formation by bacterial pathogens. *Chem Biol 19*, 1503-1513. doi:10.1016/j.chembiol.2012.10.022

Khatoon, Z., McTiernan, C. D., Suuronen, E. J. et al. (2018). Bacterial biofilm formation on implantable devices and approaches to its treatment and prevention. *Heliyon 4*, e01067. doi:10.1016/j.heliyon.2018.e01067

Kot, B., Sytykiewicz, H. and Sprawka, I. (2018). Expression of the biofilm-associated genes in methicillin-resistant Staphylococcus aureus in biofilm and planktonic conditions. *Int J Mol Sci 19*, 3487. doi:10.3390/ijms19113487

Le, K. Y. and Otto, M. (2015). Quorum-sensing regulation in staphylococci – An overview. *Front Microbiol 6*, 1174. doi:10.3389/fmicb.2015.01174

Lebeaux, D., Chauhan, A., Rendueles, O. et al. (2013). From in vitro to in vivo models of bacterial biofilm-related infections. *Pathogens 2,* 288-356. doi:10.3390/pathogens2020288

Mannala, G. K., Izar, B., Rupp, O. et al. (2017a). Listeria monocytogenes induces a virulence-dependent microRNA signature that regulates the immune response in Galleria mellonella. *Front Microbiol 8*, 2463. doi:10.3389/fmicb.2017.02463

Mannala, G. K., Hain, T., Spröer, C. et al. (2017b). Complete genome and plasmid sequences of Staphylococcus aureus EDCC 5055 (DSM 28763), used to study implant-associated infections. *Genome Announc 5*, e01698-16. doi:10.1128/genomeA.01698-16

Mannala, G. K., Koettnitz, J., Mohamed, W. et al. (2018). Whole-genome comparison of high and low virulent Staphylococcus aureus isolates inducing implant-associated bone infections. *Int J Med Microbiol 308*, 505-513. doi:10.1016/j.ijmm.2018.04.005

Moriarty, T. F., Schmid, T., Post, V. et al. (2017). A large animal model for a failed two-stage revision of intramedullary nail-related infection by methicillin-resistant Staphylococcus aureus. *Eur Cells Mater 34*, 83-98. doi:10.22203/eCM.v034a06

Moriarty, T. F., Harris, L. G., Mooney, R. A. et al. (2019). Recommendations for design and conduct of preclinical in vivo studies of orthopedic device-related infection. *J Orthop Res 37,* 271-287. doi:10.1002/jor.24230

Mukherjee, K., Altincicek, B., Hain, T. et al. (2010). Galleria mellonella as a model system for studying Listeria pathogenesis. *Appl Environ Microbiol 76*, 310-317. doi:10.1128/AEM.01301-09

Nishitani, K., Sutipornpalangkul, W., De Mesy Bentley, K. L. et al. (2015). Quantifying the natural history of biofilm formation in vivo during the establishment of chronic implant-associated Staphylococcus aureus osteomyelitis in mice to identify critical pathogen and host factors. *J Orthop Res 33*, 1311-1319. doi:10.1002/jor.22907

Paharik, A. E. and Horswill, A. R. (2016). The Staphylococcal biofilm: Adhesins, regulation, and host response. *Microbiol Spectr 4*. doi:10.1128/microbiolspec.vmbf-0022-2015

Pfaffl, M. W. (2001). A new mathematical model for relative quantification in real-time RT-PCR. *Nucleic Acids Res 29*, e45. doi:10.1093/nar/29.9.e45

Ribeiro, M., Monteiro, F. J. and Ferraz, M. P. (2012). Infection of orthopedic implants with emphasis on bacterial adhesion process and techniques used in studying bacterial-material interactions. *Biomatter 2*, 176-194. doi:10.4161/biom.22905

Russell, W. M. S. and Burch, R. L. (1959). *The Principles of Humane Experimental Technique*. https://caat.jhsph.edu/principles/the-principles-of-humane-experimental-technique

Tsang, L. H., Cassat, J. E., Shaw, L. N. et al. (2008). Factors contributing to the biofilm-deficient phenotype of Staphylococcus aureus sarA mutants. *PLoS One 3*, e3361. doi:10.1371/journal.pone.0003361

Valle, J., Vergara-Irigaray, M., Merino, N. et al. (2007). sigmaB regulates IS256-mediated Staphylococcus aureus biofilm phenotypic variation. *J Bacteriol 189*, 2886-2896. doi:10.1128/JB.01767-06

Waldvogel, F. A., Bisno, A. L. (eds.) (2000). *Infections Associated with Indwelling Medical Devices, Third Edition*. American Society of Microbiology. doi:10.1128/9781555818067

Yarwood, J. M., Bartels, D. J., Volper, E. M. et al. (2004). Quorum sensing in Staphylococcus aureus biofilms. *J Bacteriol 186*, 1838-1850. doi:10.1128/JB.186.6.1838-1850.2004

Zimmerli, W., Trampuz, A. and Ochsner, P. E. (2004). Prosthetic-joint infections. *N Engl J Med 351*, 1645-1654. doi:10.1056/NEJMra040181

Conflict of interest

The authors declare no conflicts of interest.

Acknowledgments

The authors thank Silke Zechel and Steffan Olejniczak for technical assistance.